

“There and back again” - Ultrastructural changes in the gills of Bathymodiolus vent-mussels during symbiont loss: Back to a regular filter-feeding epidermis

Bérénice Piquet, Sophie Le Panse, François Lallier, Sébastien Duperron, Ann C. Andersen

▶ **To cite this version:**

Bérénice Piquet, Sophie Le Panse, François Lallier, Sébastien Duperron, Ann C. Andersen. “There and back again” - Ultrastructural changes in the gills of Bathymodiolus vent-mussels during symbiont loss: Back to a regular filter-feeding epidermis. Frontiers in Marine Science, 2022, 9, pp.968331. 10.3389/fmars.2022.968331 . mnhn-03858445

HAL Id: mnhn-03858445
https://mnhn.hal.science/mnhn-03858445

Submitted on 17 Nov 2022

HAL is a multi-disciplinary open access archive for the deposit and dissemination of scientific research documents, whether they are published or not. The documents may come from teaching and research institutions in France or abroad, or from public or private research centers.

L’archive ouverte pluridisciplinaire **HAL**, est destinée au dépôt et à la diffusion de documents scientifiques de niveau recherche, publiés ou non, émanant des établissements d’enseignement et de recherche français ou étrangers, des laboratoires publics ou privés.

frontiers | Frontiers in Marine Science

TYPE Original Research
PUBLISHED 02 September 2022
DOI 10.3389/fmars.2022.968331

Check for updates

OPEN ACCESS

EDITED BY
Alexandra Anh-Thu Weber,
Swiss Federal Institute of Aquatic Science and Technology, Switzerland

REVIEWED BY
Xinguo Zhao,
Yellow Sea Fisheries Research Institute, (CAFS), China
Zongli Yao,
East China Sea Fisheries Research Institute, (CAFS), China

*CORRESPONDENCE
Ann C. Andersen
andersen@sb-roscoff.fr

SPECIALTY SECTION
This article was submitted to Deep-Sea Environments and Ecology, a section of the journal Frontiers in Marine Science

RECEIVED 13 June 2022
ACCEPTED 10 August 2022
PUBLISHED 02 September 2022

CITATION
Piquet B, Le Panse S, Lallier FH, Duperron S and Andersen AC (2022) "There and back again" - Ultrastructural changes in the gills of Bathymodiolus vent-mussels during symbiont loss: Back to a regular filter-feeding epidermis.
Front. Mar. Sci. 9:968331.
doi: 10.3389/fmars.2022.968331

COPYRIGHT
© 2022 Piquet, Le Panse, Lallier, Duperron and Andersen. This is an open-access article distributed under the terms of the Creative Commons Attribution License (CC BY). The use, distribution or reproduction in other forums is permitted, provided the original author(s) and the copyright owner(s) are credited and that the original publication in this journal is cited, in accordance with accepted academic practice. No use, distribution or reproduction is permitted which does not comply with these terms.

"There and back again" - Ultrastructural changes in the gills of *Bathymodiolus* vent-mussels during symbiont loss: Back to a regular filter-feeding epidermis

Bérénice Piquet[1,2], Sophie Le Panse[3], François H. Lallier[1], Sébastien Duperron[2] and Ann C. Andersen[1*]

[1]Sorbonne Université, Centre National de Recherche Scientifique (CNRS), Unité Mixte de Recherche (UMR) 7144 Adaptation et Diversité en Milieu Marin, Equipe Dynamique de la Diversité, Station Biologique de Roscoff, Roscoff, France, [2]Muséum National d'Histoire Naturelle, Centre National de Recherche Scientifique (CNRS), Unité Mixte de Recherche (UMR) 7245 Molécules de Communication et Adaptation des Micro-organismes, Paris, France, [3]Centre National de Recherche Scientifique (CNRS), Sorbonne Université, FR2424 Plateforme MerImage, Station Biologique de Roscoff, Roscoff, France

Deep-sea mussels *Bathymodiolus azoricus*, from Azorean hydrothermal vents, house two types of symbionts in their fleshy gills: methane-oxidizing (MOX) and sulfide-oxidizing (SOX) Gamma-proteobacteria. As soon as the mussels are collected, their symbionts are deprived from their environmental nutrient flux, and cannot rely on their usual metabolism. Recent studies have shown that the gill cells undergo high rates of apoptosis, as well as regionalized cell proliferation. This study follows the fate of the symbionts and of the hosting bacteriocytes at the ultrastructural level, during an extended starvation period. Just upon collection, we evidenced an apico-basal journey of the symbionts in the bacteriocytes, starting with (1) apical single symbiont endocytosis, (2) symbiont division, (3) symbiont storage, (4) and symbiont digestion within lysosomes, above the basal lamina. After 4-9 days starvation, endocytosis occurred with (5) empty blebbing, (6) the lysosomes increased in size, and the bacteriocytes lost their apical membrane, resulting in (7) a baso-apical return of the symbiont-containing lysosomes outside the gills, while the nucleus showed condensed chromatin, characteristic of apoptosis/necroptosis (8). Between the bacteriocytes, narrow intercalary cells appear to divide (9). Our hypothesis is that intercalary cells are stem cells that replace lost bacteriocytes. After 61 days there was no symbiont left, and the epidermis resembled those of the non-symbiotic filter-feeding mussel Mytilus edulis.

KEYWORDS

symbiosis, bivalves, Modiolinae, hydrothermal vents, gill ultrastructure, transmission electron microscopy, ultrastructural gill changes

Introduction

Deep-sea mussels *Bathymodiolus* spp., living at cold seeps or at hydrothermal vents, are unique in the way they associate with chemosynthetic bacterial symbionts that ensure most of their nutrition, (for review see Duperron 2006, Duperron 2010; Laming et al., 2018). Despite belonging to the family Mytilidae, and phylogenetically deriving from shallow ancestors that probably resembled coastal mussels like *Mytilus edulis* (Distel et al., 2000; Little and Vrijenhoek, 2003; Lorion et al., 2013), *Bathymodiolus'* gills have evolved to shelter dense populations of bacteria within specialized epithelial cells: the bacteriocytes. The number of endosymbiotic bacteria found within the gills of *B. puteoserpentis* is estimated to be about $2.5x10^{12}$ per individual (Duperron et al., 2016), which represents as many bacteria as those found in one cubic meter (i.e. 1 000 L) of seawater. Thus, the deep-sea mussels are able to concentrate their symbionts within their gills, and this explains why their gills are so thick and fleshy. The symbionts are either sulfide-oxidizing (SOX) or methane-oxidizing (MOX) Gamma-proteobacteria, and some *Bathymodiolus* species house both (Childress et al., 1986; Brooks et al., 1987; Fisher et al., 1987; Cavanaugh et al., 1992). Additional symbiont types have been identified, but usually in low abundances (Zielinski et al., 2009; Raggi et al., 2013; Assié et al., 2016). *Bathymodiolus* acquire their symbionts just after their larval metamorphosis, at the plantigrade settlement stage, and this triggers the differentiation of their gill epithelium into a symbiont containing organ (Laming et al., 2018; Franke et al., 2020). Symbionts can either be acquired from the surrounding environment (i.e. horizontal transfer) and/or be escaped symbionts from nearby *Bathymodiolus* (i.e. lateral transfer), (Won et al., 2003; Wentrup et al., 2013; Franke et al., 2020). During mussel growth, the gills continuously grow in length at their posterior end. The newly-formed posterior gill lamellae initially appear devoid of symbionts, which can be acquired throughout the whole life of the mussel host (Wentrup et al., 2014). The acquisition seems to involve a recognition process of the bacterial symbionts by several Peptidoglycan Recognition Proteins (PGRPs) that are expressed by the gill tissue (Détrée et al., 2017). After binding to the epithelium at the level of the bacteriocytes microvilli (Le Pennec et al., 1988), the bacterial symbionts are likely internalized as both Toll like receptor (TLR13) and two adhesion gene families: syndecan and protocadherin, reported to mediate endocytosis, are expanded in the genomic repertoire of *B. platifrons* (Sun et al., 2017). Endocytosis/phagocytosis might occur through open pit-like structures in the cell membrane of the gill surface (Won et al., 2003; Kádár et al., 2006). A recent study proved phagocytic activity of the epidermal cells engulfing indiscriminately exogeneous bacteria, and suggest an inside regulation to discriminate and keep the true symbionts, located intracellularly within vacuoles (Tame et al., 2022). It appears that all the membranous chambers housing symbionts within a single bacteriocyte of *B. septemdierum*, are interconnected together and also connected with the external environment (Ikuta et al., 2021). This later study questions whether the symbiosis is really intra- or extra-cellular, in particular because extracellular symbioses are reported in various genera within the Bathymodiolinae (Duperron et al., 2008; Fujiwara et al., 2010; Halary et al., 2011).

The fate of the symbionts within their host is still a matter of debate, and two different pathways have been discussed: *Bathymodiolus* could get organic carbon compounds either by "farming", (Fisher and Childress, 1992; Fiala-Medioni et al., 1994; Streams et al., 1997), or by "milking" their symbionts (Kádár et al., 2008). "Farming" corresponds to the digestion of bacterial symbionts, while "milking" means that the symbionts could be leaking low-weight metabolites (sugar or amino acids) to the host, but avoiding being themselves digested by the host, as formerly documented in corals (Muscatine et al., 1981). Symbionts are known to be lost if their necessary substrate (sulfide or methane) is not available anymore. This has been documented in several experiments, where vent or seep mussels have been maintained in laboratory aquaria for one to 6 months (Kádár et al., 2005; Bettencourt et al., 2008). However, since sulfide or methane are vital to sustain the symbionts, what we observe in the gills once the mussels are collected and kept in surface sea-water on board, is already the initiation of a starvation process for their symbionts, and their hosts' gill cells response to this process. In the gills of *B. azoricus*, we have recently shown high rates of apoptosis, especially in the abfrontal regions of gill filaments where symbionts are less abundant, as well as regionalized cell proliferation occurring sporadically along the gill filaments and in the same zones where apoptosis was localized (Piquet et al., 2019; Piquet et al., 2020). Since pressurized/unpressurized ways of collection did not alter the percentage of apoptosis, this high rate of apoptosis cannot be a depressurization artefact upon collection, but must be a special feature in *Bathymodiolus* mussels, to which regionalized cell proliferation might be a compensation. Thus, what occurs at the ultrastructural level when starvation is initiated and extended, and which has not previously been thoroughly documented, needed further exploration.

The present work aims to document the stages of symbiont loss at the ultrastructural level, and how the gill epidermis deals with a forced non-symbiotic state. We monitored the ultrastructure of vent mussel gills and associated bacterial symbionts over a 61 days starvation experiment conducted on *B. azoricus* collected from a shallow hydrothermal vent site (Menez Gwen) and a deeper vent site (Lucky Strike). We used the coastal blue mussel *Mytilus edulis* as cytological comparative reference for a non-symbiotic mussel gill epithelium. Besides the pathways of

symbiont loss, our aim is also to document the fate of the symbiont-free host cells and associated modifications in their ultrastructure. We hypothesize that symbiont loss is due to (1) enhanced symbiont digestion, followed by bacteriocyte dedifferentiation, i.e. differentiation into a non-symbiotic cell type or (2) bacteriocyte destruction (resulting in symbiont loss) and bacteriocyte replacement by a new cell that does not contain symbionts, possibly restoring a pre-infection type of epidermis. The latter hypothesis supports the idea that a non-fed symbiont could ultimately become heterotroph, and possibly have a negative impact on the host cells, i.e. become a "parasite". Thus, the host might get rid of its starving symbionts, either by digestion (lysosomes) or by destruction of the symbiont-containing host cell (which could explain the high level of apoptosis).

Material and methods

Specimen collections

Specimens of *Bathymodiolus azoricus* were collected during the MOMARSAT/BioBaz 2017 cruise (Sarradin and Cannat, 2017; Lallier 2017). Specimens were sampled at the Menez Gwen shallow hydrothermal vent site (MG2 marker; 37°50.669 N; 31° 31.156 W, - 830m depth) and at the deeper site Lucky strike, close to the marker "Tour Eiffel" (37°17.341 N; 32°16.542 W; -1693 m depth). Mussels were sampled by the ROV Victor 6000, and brought to the surface in hermetic boxes. TEM imagery analysis is based on 7 specimens from Menez Gwen and 3 from Lucky Strike (see below). *Mytilus edulis* were collected in Bloscon harbor at Roscoff (48°42.975 N, 3°57.835 W, mean shell length: 47.3 ± 2.0 mm), for comparison with a non-symbiotic gill epidermis.

Maintenance of the mussels at the laboratory

Recovered *Bathymodiolus azoricus* specimens were transferred to surface seawater aquaria on board at a temperature of 8°C, which corresponds to the *in situ* seawater temperature at Menez Gwen where the mussels where collected (Colaço et al., 1998). The mussel gills (from Lucky Strike and Menez Gwen) at t=0 were dissected at 8°C within 10 minutes after recovery and fixed on board. Four days after collection (t=4 days), mussels from Menez Gwen transferred to Lab Horta (Azores) were fixed at 8°C. The remaining collected mussels from Menez Gwen were transferred by airplane to the aquaria of Océanopolis in Brest (France). The mussels were kept unfed at 8° ± 2°C and at atmospheric pressure in local natural seawater filtered at 0.22 µm and then 0.1µm for a duration of 7, 9, 16, and 61 days. For all mussels the mean shell length was: 42.9 ± 3,9 mm. *Mytilus edulis*, within the same size range as *Bathymodiolus*, were maintained in *Roscoff Aquarium Service* (RAS, 8°C, filtered natural seawater) 36h without food until processing.

Fluorescence *in situ* hybridization

Gill fragments were fixed in 4% formaldehyde in sterile-filtered seawater (SFS) for 2 hours. They were then rinsed in natural filtered seawater, and dehydrated in increasing series of ethanol (50, 70 and 80%, 15 min each). In the laboratory, gills were embedded in polyethylene glycol (PEG) di-stearate: 1-hexadecanol (9:1), cut into 8 µm-thick sections using a microtome (Thermo, Germany), recovered on SuperFrost Plus slides (VWR International, USA), and stored at -20°C. Fluorescence *in situ* hybridization (FISH) experiments were performed to confirm the localization of symbionts using the probes described previously (Szafranski et al., 2015). Shortly, resin was removed using ethanol prior to hybridization. Hybridization procedure was performed as described previously (Piquet et al., 2018, Piquet et al. 2019) using FITC; Cy-3 and Cy-5 labeled probes ImedM-138 (5'-ACCAGGTTGTCCCCCACTAA-3') (Duperron et al., 2008), specific for methanotrophic symbionts, and probe BangT-642 (5'- CCTATACTCTAGCTTGCCAG-3') specific for sulfide-oxidizing symbionts, (Duperron et al., 2005); for 3 hours at 46°C in a 30% formamide-containing buffer. Hybridized gill sections were visualized under a SP5 confocal microscope (Leica, Germany).

Transmission electron microscopy

Gill filaments were fixed overnight at 4°C in a 0.2 M cacodylate buffer solution (pH 7.2) containing 4% glutaraldehyde and 0.95% NaCl. The gills were then rinsed in a 0.2 M cacodylate buffer solution pH 7.2 containing 2.25% NaCl. Samples were then stored at 4°C until further processing.

Back to the laboratory, samples were rinsed with cacodylate buffer and post-fixed with 1% osmium in cacodylate buffer for 1 hour. After two rinses with cacodylate buffer, the samples were dehydrated in increasing ethanol series (50%-70%-95%, and 100% ethanol; 3 x 20 minutes each). The impregnation was made in successive mixtures of 100% ethanol and Spürr resin (1/3, 1/2 and 3/1, during one hour each, and overnight for the last). Then, three pure Spürr resin baths of 3 hours for the first two, followed by a night for the last bath, were carried out. Finally, polymerization took place in an oven at 60°C for two days.

Blocks were cut with an ultra-microtome (LEICA Ultracut UCT Microtome), and 60 nm-thick sections were contrasted with 2.5% uranyl acetate and 0.2% lead citrate, and observed under a JEOL 1400 TEM. Structures and organelles were

measured directly on the TEM using a dedicated measurement tool.

Results

Symbiont loss visualized with FISH

Symbiont loss was visible to the naked eye in the starved *Bathymodiolus*, because after 61 days, the gills had changed color, from brown to creamy white, and shape, from thick to thin lamellae (Figures 1A, B). Although the gills had lost in thickness, no mortality was observed during the 61 days maintenance period in Roscoff's Aquarium Service. Moreover, all mussels were quite actively moving within the tank (see video V1 in Supplementary Material).

Preliminary overview of symbiont densities was obtained using FISH, based on specimens from days 0, 1, 2, 4, 5, 6, 7, 8, 9, 16, and 61, observed on several gill filaments per time point. In total, 17 individuals were observed from which 11 from Menez Gwen and 6 from Lucky Strike, with 3 sections per individual, i.e. 42 sections in total. It confirmed that symbiont densities overall decreased with time in the lateral and abfrontal zones, while the frontal zone always remained devoid of symbionts. Control specimens analyzed immediately upon recovery displayed bacteriocytes packed with SOX and MOX symbionts (Figure 2A). Their abundance seemed to vary from one bacteriocyte to another and along the gill lamellae, with lower bacterial densities in bacteriocytes located in the abfrontal zone of the filament, i.e. opposite to the frontal inhalant seawater current (Figure 2A). After 8 days devoid of substrates to the symbionts, both symbiont types were still visible, yet in lower abundance and mainly restricted to the surface of the gill cells, i.e. to the most apical pole of the bacteriocytes (Figure 2B). After 16 days starvation, a few symbionts were still sporadically observed in a few bacteriocytes (Figure 2C), but after 61 days, no symbiont was visible anymore in any of the bacteriocytes examined (Figure 2D).

Ultrastructural modifications of the bacteriocytes during starvation

Upon mussel recovery, TEM views of the gill epidermis of *B. azoricus* from the shallow vent site Menez Gwen (Figure 3A), and from the deeper Lucky Strike site (Figure 3B) confirmed that symbionts were almost filling the entire cytoplasm of the bacteriocytes. The fronto-lateral bacteriocytes, measured from their apex to their basal limit with the basal lamina, were about 35 µm (34.85 ± 5.76 µm, *n=8 bacteriocytes*), which is within the same range as the frontal ciliated cells (31.41 ± 2.13 µm, *n=6*) (*n* being the number of measurements taken on bacteriocytes from several pictures). When the bacteriocytes were full of symbionts, their apical cytoplasmic membrane generally appeared quite smooth (Figure 3A) or with only very few apical microvilli visible (Figure 3B). Moreover, the bacteriocytes were apically segregated from the neighbor cells, by tight junctions (Figure 3B). At the very apex of the bacteriocytes, the symbiotic bacteria often occur as single (boxed n°1 on Figures 3A, B and 4A, B), but occurred clustered in vacuoles further down the bacteriocytes. In the seven individuals we examined from Menez Gwen, SOX and MOX symbionts were located in distinct vacuoles (Figures 3A, 4A, C, E, G), whereas in the three specimens we observed from Lucky Strike, MOX and SOX symbionts were often co-occurring together within the same vacuole (Figures 3B, 4 F, H). A few SOX appeared very long

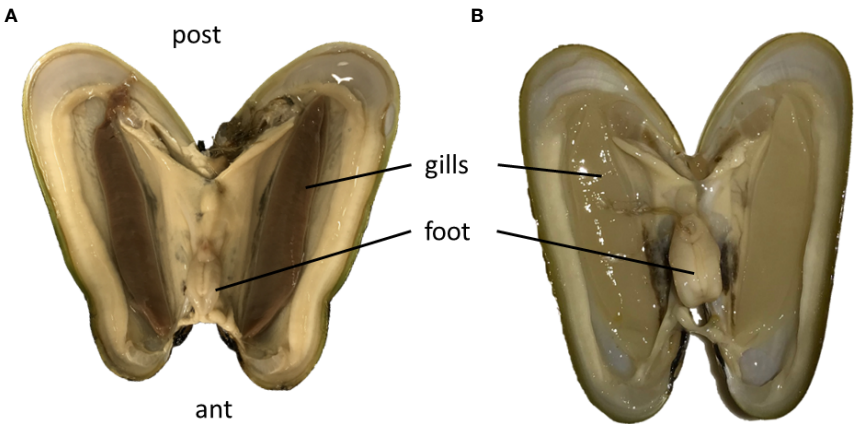


FIGURE 1
Open mussels of *B azoricus* with their pairs of thick brown gills just upon collection **(A)**, which become translucent and thin after 61 days of starvation **(B)**. Ant, anterior part of the mussel shell; post, posterior part of the mussel shell; The shells measured about 4 cm in length. **(A)** is modified from Piquet et al., 2019 in Plos One with permission.

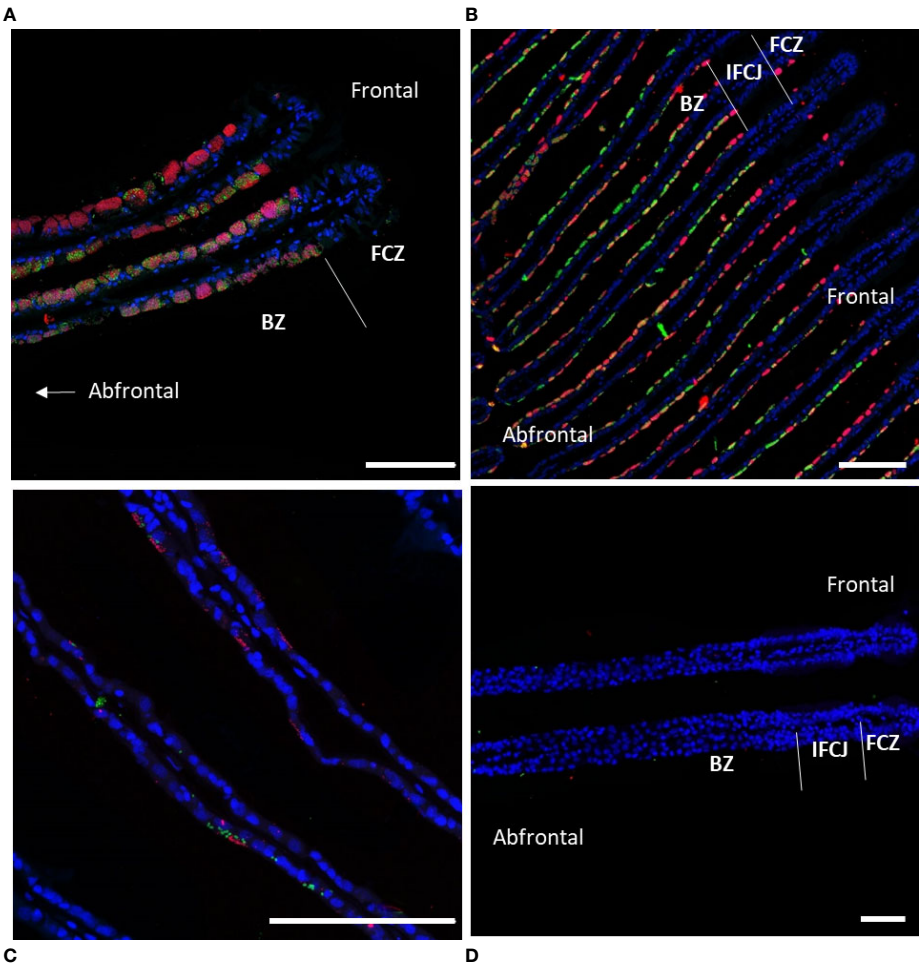


FIGURE 2
Fluorescence *in situ* hybridization performed on gill lamellae cross-sections showing decreasing symbiont densities during starvation. Host nuclei stained by DAPI in blue, Methane-Oxidizing symbiont (MOX) in green, and Sulfide-Oxidizing symbiont (SOX) in red. **(A)** Immediately after collection (t=0), MOX and SOX fill almost the entire cytoplasm of all bacteriocytes; **(B)** after 8 days of starvation MOX and SOX are restricted to the cytoplasmic apex of the bacteriocytes; **(C)** after 16 days, MOX and SOX are only present sporadically in the apex of some bacteriocytes; **(D)** after 61 days of starvation MOX and SOX have almost totally disappeared from the gill epidermis. Abbreviations: BZ bacteriocyte zone, FCZ frontal ciliated zone, IFCJ inter-filamentary ciliated junctions. The abfrontal zones correspond to the inner side of the gill lamellae, opposite to the frontal ciliated zones, the latter corresponding to the external sides of the gill lamellae facing the inhalant sea-water current (see Figure 1A in Piquet et al., 2020, for a three-dimensional scheme). All Scale bars represents 100 µm.

with a narrowing in their middle region giving them the typical 8-numbered shape of a bacterium undergoing division inside the vacuole (boxed n°2 on Figures 3A, B and 4D). Rare MOX also appeared to be dividing (Figure 4C). Dividing stages were generally seen below the apical cell membrane, or at least in the apical third of the bacteriocyte (boxed n° 2 on Figures 3A, B), as if it occurred soon after the symbiotic bacteria were phagocyted. At both sites, the symbionts appeared in increasingly large clusters, the more basally they were located in the bacteriocyte (boxed n° 3 on Figures 3A, B). Above the basal lamina, Figure 3A shows large lysosomal vesicles (boxed n° 4 on Figures 3A, B), containing membrane whorls of onion-peel structures around elements resembling degraded symbionts (Figure 4G). At Lucky Strike, more or less degraded MOX and SOX occurred together within lysosomal vesicles, indicating they were also digested together (Figure 4H). Finally, the nucleus of each bacteriocyte was generally located basally, surrounded by a few rows of rough endoplasmic reticulum (Figures 3A, B), just above the basal lamina.

We randomly sampled some of the mussels from the maintenance tank and fixed their gills at specific time points. During the early time of starvation, at days d4, d7 and d9, the ultrastructure of the bacteriocytes displayed strong similarities, therefore we chose to illustrate similar cell processes from either

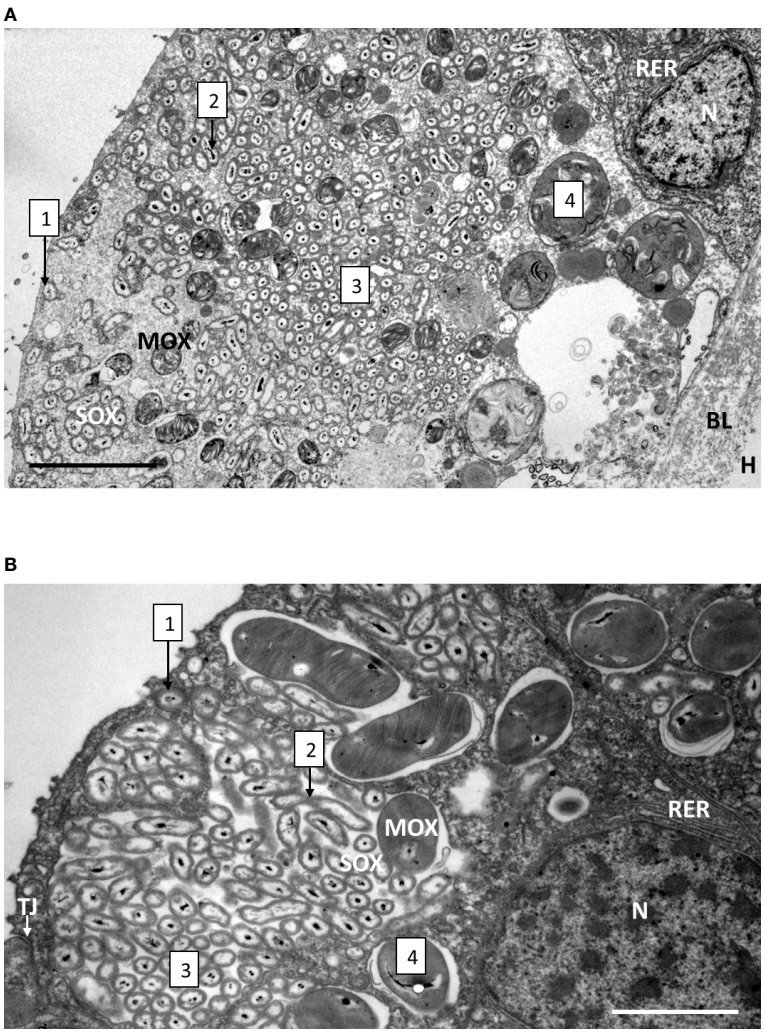


FIGURE 3
Gill epidermis immediately upon recovery, showing the bacteriocytes of *B azoricus* from Menez Gwen **(A)** and from Lucky Strike **(B)**. The boxed numbers on the microphotograph refer to the successive events, localized from the cellular apex (to the left on the pictures) to the basal lamina (to the right on the pictures), and detailed as follows: 1- Apical endocytosis of single symbionts (SOX or MOX) from the inhalant seawater flow. 2- Symbiont division. 3- Symbiont storage in vacuoles. 4- Symbiont digestion in the basal region of the bacteriocyte. Note that in *B. azoricus* from Menez Gwen **(A)** MOX and SOX appear segregated in separate vacuoles, while they share the same vacuoles in the mussels from Lucky Strike **(B)**. Abbreviations: BL basal lamina, H hemolymph, MOX methane-oxidizing symbiont, N nucleus, RER rough endoplasmic reticulum, SOX sulfide-oxidizing symbiont, TJ tight junction. Scale bars represent 5 µm in **(A)** and 2 µm in **(B)**.

of these early starvation times in Figures 5, 6. The most noteworthy observations were the occurrence of numerous microvilli at the apical plasma membrane of the bacteriocytes (Figures 5A–E). An empty blebbing gave a spongy aspect to their apical part (Figures 5A–C). Lysosomes are initially basally-located, and when increasing in size, they tend to occupy almost the entire bacteriocyte (Figures 5C, D). A new event is shown at d9, (even if it also was observed earlier): between two intact intercalary cells, some single bacteriocytes appeared totally devoid of apical cell membrane and were missing most of their cytoplasmic content (Figure 5E). At their base, the nucleus showed the dark chromatin condensed at its periphery (Figures 5E-G) and sometimes also buddings of the nuclear envelope (Figure 5F).

During the first week of starvation, we also noticed several signs of cell divisions (Figure 6). For instance, a bacteriocyte that did not show apical blebbing, but still contained symbionts, showed a dividing nucleus appearing elongated and slightly 8-shaped with two nucleoli (Figure 6A). Beside this bacteriocyte, a narrow intercalary cell, characterized by not containing symbionts, but mitochondria, had a regular vertically oriented nucleus within the gill filament. On the

10.3389/fmars.2022.968331

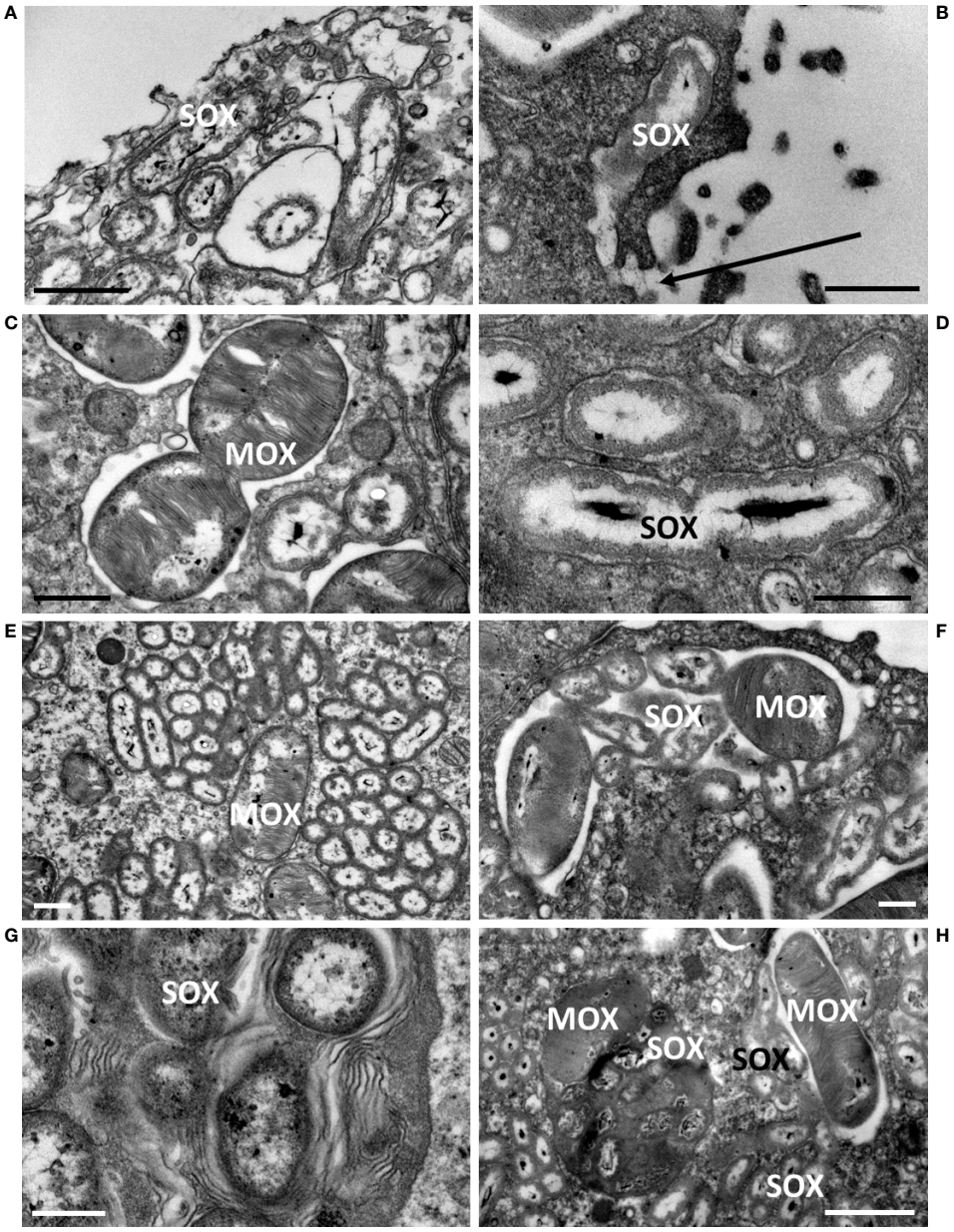


FIGURE 4
Close-up details of bacteriocytes in *B azoricus* from Menez Gwen (left column) and from Lucky Strike (right column), immediately upon recovery, illustrating the four processes (numbered according to the successive processes shown as boxed numbers on Figure 3. (1) **(A, B)**,apical endocytosis, (2) **(C, D)**, symbiont division, (3) **(E, F)**, symbiont storage, (4) **(G, H)**, symbiont digestion. In A and B, the apical microvilli and the endocytic vacuoles phagocyte a single bacterium, here a SOX symbiont. A direct connection between the vacuole and the external seawater is visible in **(B)**, and pointed by an arrow. **(C)** Division of a MOX symbiont displaying the two daughter bacteria. **(D)** Division of a SOX symbiont with the two daughter nucleoids appearing clearly segregated, while they were still not separated by a bacterial wall. **(E, F)** Vacuoles contain either SOX or MOX in **(B)** *azoricus* from Menez Gwen **(E)**, but both types of symbionts share the same vacuole at Lucky Strike **(F)**. **(G, H)** the most basal vacuoles contain onion-peel membranes **(G)** and/or degraded SOX/MOX symbionts **(H)** indicating they are putative lysosomes digesting symbionts. Scale bars represent 0.5 µm in **(B, D, F, G)**; 1 µm in **(C–E)** and 2 µm in **(H)**.

contrary, the more the bacteriocytes had empty blebbing out-pocking above the apical surface of the gill lamellae, the more the flanking intercalary cells showed to occur pairwise with their nuclei tightly close to one another, resembling a mother cell that recently had undergone division into two daughter cells. Moreover, these nuclei within the gill filament, showed a marked oblique orientation, below the out-pocking bacteriocyte (Figures 6B–D). After 7 days starvation, the

10.3389/fmars.2022.968331

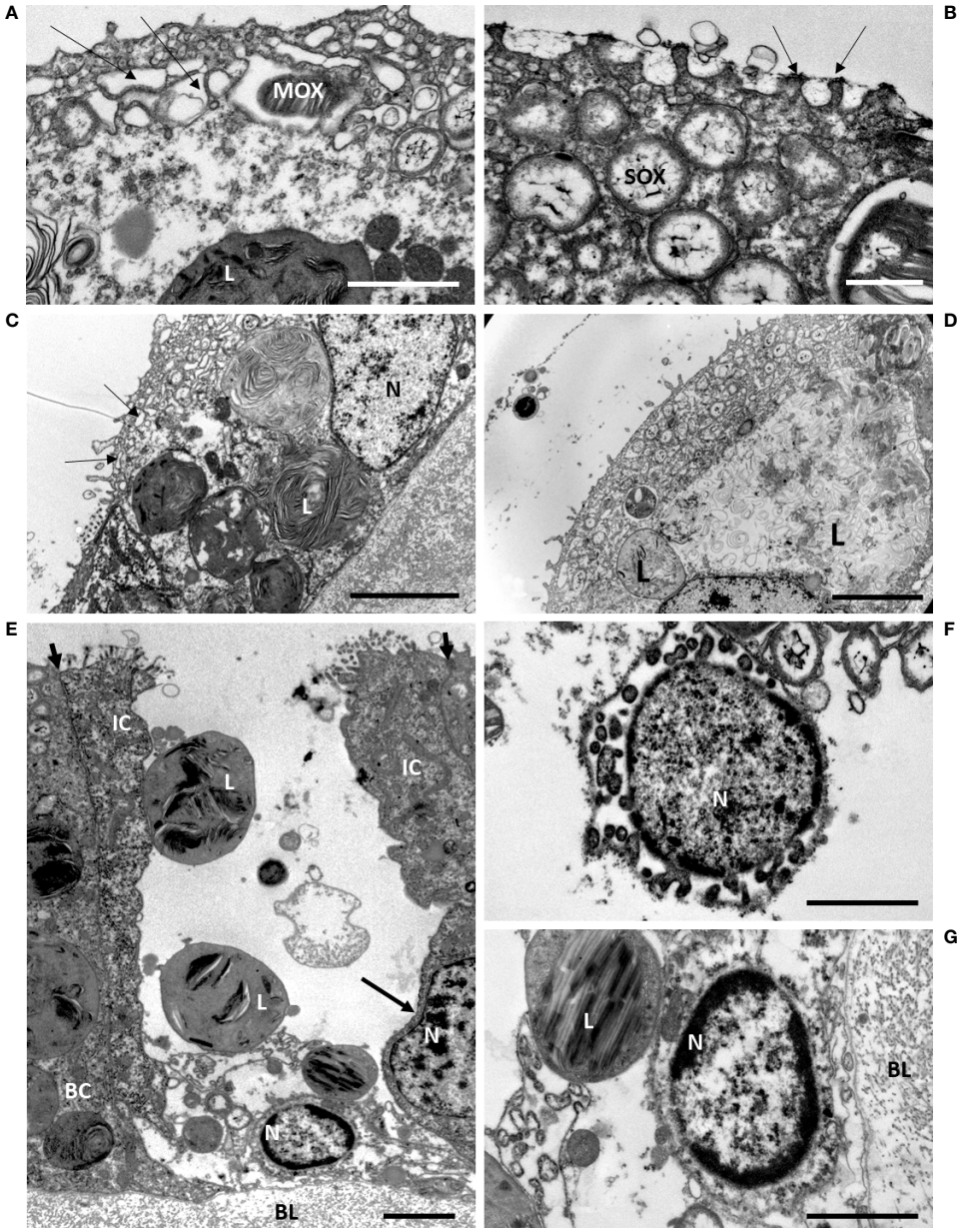


FIGURE 5
Early starvation effects on gill epidermis in *B azoricus*, at Menez Gwen, days d7 **(A, C, D)** and d9 **(B, E, F, G)**. On the figures **(A–D)**, many microvilli are present at the apical surface of the bacteriocyte. Note that they often bend towards each other, two by two, as pointed by the arrows in **(B)**. **(A–C)** the upper layer of the epidermis shows apical blebbing pointed by arrows in **(A, C)** i.e. phagocytic vacuoles that appeared empty, above a deeper layer of vacuoles containing a few symbionts. **(C, D)** the lysosomes containing onion-peel structures increase in size towards the basal part of the bacteriocytes. The symbiont shapes appear more or less recognizable on C (d7), but are much looser on D (d7); **(E)** this single bacteriocyte is missing its apical cell membrane and most of its cytoplasm, but still having some large lysosomes and its basal nucleus with condensed chromatin. This bacteriocyte is framed by two intact intercalary cells. The apical short arrows point to the tight junctions between each intercalary cell and their next neighbor cell and underline their narrowness. The intercalary cell to the right has an 8-shaped nucleus (long arrow) indicating it was possibly in the process of division. **(F)** Detail of another empty bacteriocyte with its nucleus showing condensed chromatin and budding at is periphery. **(G)** Close view of the basal nucleus with peripheric condensed chromatin shown in **(E)**. BC, bacteriocyte; BL, basal lamina; IC, intercalary cell; L, lysosome; MOX, methane-oxidizing symbiont; N, nucleus; SOX, sulfide-oxidizing symbiont. Scale bars represent 2µm in **(A, B, F, G)** and 5 µm in **(C, D, E)**.

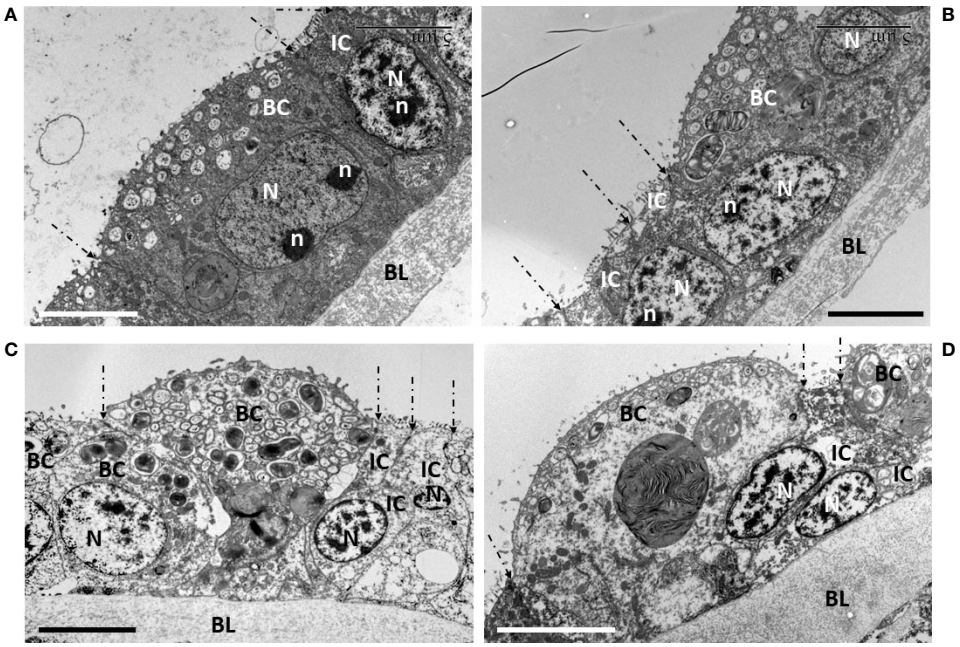


FIGURE 6
Signs of cell division during early starvation (d4, d7, d9). On all pictures, the limits between each cell are highlighted by dashed-lined arrows pointing to their apical tight-junctions. **(A)** a bacteriocyte at d7 that still contains symbionts and has no apical blebbing, shows an 8-shaped nucleus with two nucleolar masses, indicating the process of nuclear division was ongoing in this bacteriocyte. The neighboring intercalary cell and its nucleus occur in the same axis as this bacteriocyte, i.e. perpendicularly to the basal lamina. **(B–D)** focus on the narrow intercalary cells flanking the bacteriocytes that are apically blebbing and more or less out-pocking above the apical surface of the gill filament. **(B, D)** the two narrow intercalary cells show their nuclei, very close to one another, suggesting they have recently divided. In addition, the more the bacteriocyte is out-pocking, the more the position of the nucleus in each intercalary cell bends obliquely towards the basal lamina, below the bacteriocyte. **(B, D)** (d7), **(C)** (d4). BC, bacteriocyte; BL, basal lamina; N, nucleus; n, nucleolus; IC, intercalary cell. Scale bars all represent 5 µm.

remaining intact bacteriocytes had lost about two thirds of their apico-basal height, measuring 11.87 ± 1.69 µm (*n=6*).

After 61 days starvation (Figures 7A, B), the gill epidermis became very thin: the fronto-lateral cells measured only about one quarter of their initial height (8.01 ± 0.80 µm, *n= 3*), (Figure 7A), but this is still twice the height of the cells measured in the abfrontal zone (4.37 ± 1.51 µm, *n=14*) (Figure 7B). The abfrontal zone compensated its thinness with a very thick basal lamina (5.45 ± 2.31 µm, *n= 5*) (Figure 7B), which represented more than twice its thickness in the frontal area (2.54 ± 0.45 µm, *n=7*). The epidermal cells were almost cubic and devoid of symbionts, they had a reduced cytoplasm-to-nucleus area (Figure 7A). The cells looked very much alike the gill epidermis of the coastal *M. edulis* (Figures 7C, D). The gill epidermis of *Mytilus* varies from 3.5 µm in its linear lateral part and increases up to about 17 µm at the level of the frontal and latero-frontal ciliated areas (mean: 9.28 ± 4.37 µm, *n=11*). Where the epidermis is thinner in *M. edulis*, the basal lamina is also quite robust (mean: 5.07 ± 0.91 µm, *n=3*). Thus, the epidermis of *Bathymodiolus* devoid of symbiont has a thickness in the range of its non-symbiotic filter-feeding relative.

Discussion

As soon as *Bathymodiolus* mussels are collected from their deep-sea habitat, their symbionts lack the necessary sulfides/methane requested for their maintenance. Our two months long starvation experiment on *B. azoricus* shows that symbiont loss is progressive, since some cells still harbor symbionts after 16 days, but after 61 days no symbiont was detectable in the gill cells. Kádár et al. (2005) also documented a gradual disappearance of bacteria from *B .azoricus*, and quoted that no symbiont was detectable at day 30, although they supposed that some residual symbionts might have survived, as this population increased when exposed in a sulfide flux close to other symbiont-bearing mussels allowing a lateral symbiont transfer. Later works suggest a possible alternative (yet not exclusive of the former), in which epithelial cells can reacquire symbionts from the environment or neighboring gill filaments (Wentrup et al., 2014). Bettencourt et al. (2008) showed that after 3 months in sulfide-free conditions, mucus-like granules in mucocytes in *B. azoricus* were greatly reduced, but that after 6 months, their hemocytes were still capable of phagocytosis. All these experiments underline how resilient the deep-sea *Bathymodiolus* from

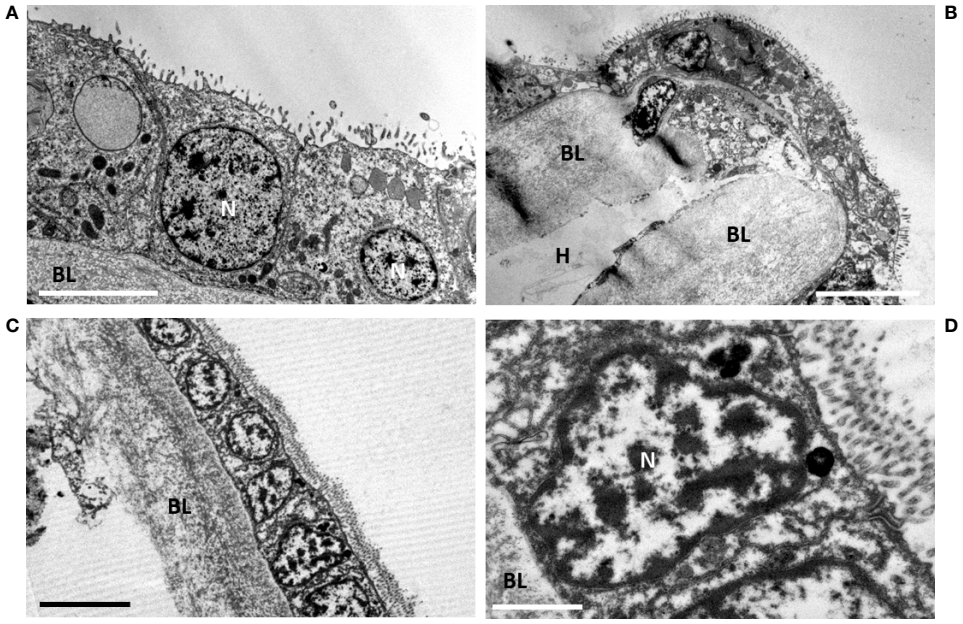


FIGURE 7
Late starvation (d61) in gill epidermis after final symbiont loss, compared with gill epidermis of the non-symbiotic coastal mussel *Mytilus edulis*. **(A)**- At d61 the gill epidermis is totally devoid of symbiont. The cells have a cubic shape and a reduced height with generally a high volume-ratio of nucleus to cytoplasm. Apically the microvilli are very developed. **(B)** Abfrontal loop showing the shrinked epidermis (≈ 2-4 µm cell height at d61, being thinner than the basal lamina (≈ 7 µm). **(C)** *Mytilus edulis* filter-feeding epidermis. **(D)** detail of a filter-feeding cell of *Mytilus edulis*, shoving the importance of its nucleus compared to the cytoplasmic area. BL, basal lamina; N, nucleus; H, Hemolymph. Scale bars represent 5 µm in **(B, C)**, 2.5µm in **(A)** and 1 µm in **(D)**.

Menez Gwen are, and this makes the investigation of the ultrastructural supports for this resilience the more interesting.

The apico-basal journey of the symbionts into the bacteriocytes

Just upon collection, the apical membrane of the bacteriocytes appears rather smooth and their apical third is full of symbionts. In *B. azoricus* from Menez Gwen, SOX and MOX are located in distinct vacuoles, as also observed by Kádár et al. (2005). However, the two symbiont types co-occur within the same vacuoles in *B. azoricus* from Lucky Strike. Bacteriocytes in *Bathymodiolus* from both sites, show apical tight junctions. Tight junctions prevent lateral diffusion of membrane proteins and thereby help to maintain an apico-basal polarity in the cells. In mammals and *Drosophila* fruit fly, tight junction proteins are even involved in cell proliferation and differentiation (Shin et al., 2006). Very often just below the apical surface, or in the upper third of the bacteriocyte we saw SOX and MOX symbionts dividing, also at d7-d9, indicating that, even deprived of nutrients, the symbionts were still alive and active, possibly relying on alternative metabolisms such as heterotrophy. More basally in specimens from Menez Gwen, SOX are grouped in particularly large clusters and MOX seem to occur by 2,3 or a few more, in grey vacuoles, indicating that they also are digested, so we suppose these vacuoles with onion-peel-like structures constitute secondary lysosomes. Secondary lysosomes usually contain membranes or particles that are in the process of digestion, they result from the fusion of one or several small spherical enzyme-containing primary lysosomes with a damaged organelle or a vacuole, (Alberts et al., 2002). Then, these large lysosomes apparently also fuse together, and at d7-d9 of starvation, lysosomes often almost fill the entire bacteriocyte. This process seems to indicate intracellular digestion, corresponding to the "farming" of symbionts, which stands in line with previous observations by several authors (Fisher and Childress, 1992; Fiala-Medioni et al., 1994; Streams et al., 1997). If digestion is complete, small molecules (sugar, amino-acids…) may leak out from the big lysosomes in close contact with the basal lamina, and be transferred to the hemolymph across the basal lamina. The basal lamina, generally made of collagen, laminin and various other proteins, is secreted by the epidermal cells, and forms a network that is not only acting as a supporting barrier, but also as a filter for molecular transfer, with a permeability that

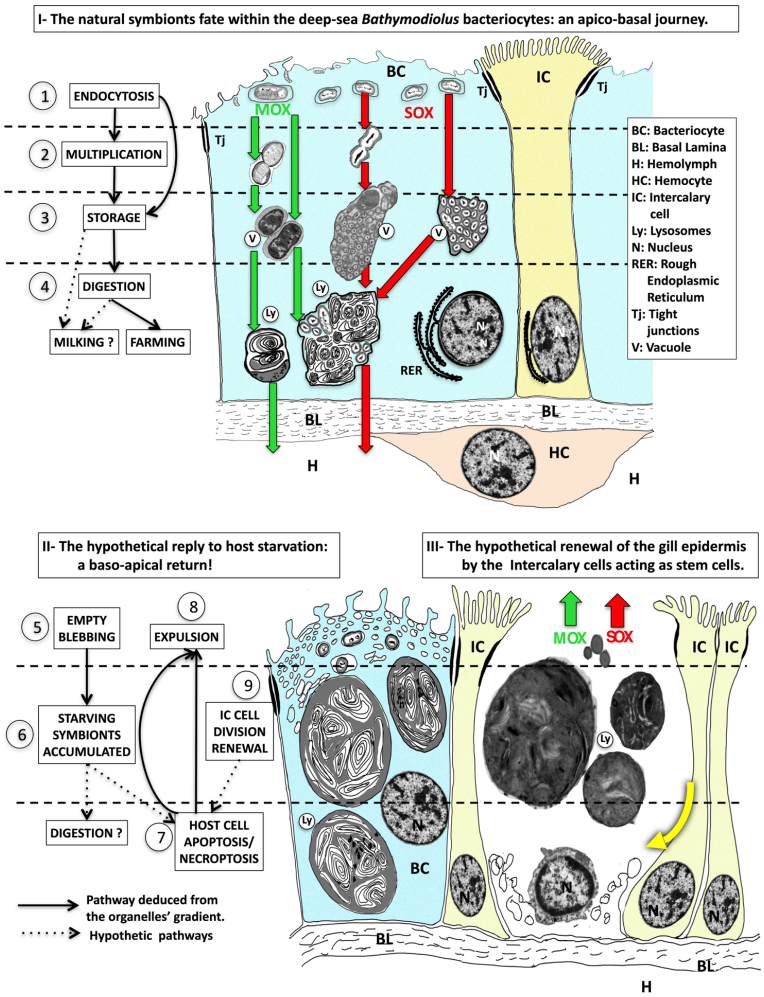


FIGURE 8
The interpreted model of the forth and back trafficking of the symbionts and their host cells during symbiont starvation. - Part I - Hypothetical apico-basal pathway when symbionts are present in the bacteriocytes, with the successive steps 1) endocytosis of the symbionts, 2) symbionts multiplication, 3) symbiont storage in vacuoles, 4) symbionts digestion in lysosomes, which leads to either digestion (i.e. farming) and/or leakage of small molecules that crosses the basal lamina and reaches the hemolymph (i.e. milking). MOX (green arrows) and SOX (red arrows) symbionts are stored in separate vesicles in *B azoricus* from Menez Gwen, (left green and red arrows), but together in mixed vacuoles in *B puteoserpentis* from Lucky Strike (right green and red arrows). The nucleus of the bacteriocyte is basal surrounded by rough endoplasmic reticulum. Intercalary cells are colored in yellow, and hemocytes in pale brown. Part II - The hypothetical response to host starvation leading to 5) empty blebbing, 6) accumulation of starving and destroyed symbionts, 7) Host cell apoptosis/necroptosis and expulsion (8). Part III Finally, intercalary cell division (9) and cellular movements (thick yellow curved arrow) below the missing bacteriocyte suggest intercalary cells might be the stem cells that enable gill epithelial renewal. The real sources of these schemes correspond to frequently observed and photographed cell features, The real sources of these schemes correspond to frequently observed and photographed cell features: step 1 see Figures 4A, B; step 2 see Figure 4C, D; step 3 see Figures 4E, F; step 4 see Figures 4G, H; step 5 see Figures 5A, B, step 6 see Figures 5C, D; step 7 & 8 see Figures Figure 5E–G; step 9, see Figures 6A, B.

might have a certain selectivity (Arends and Lieleg, 2016). Thus, it is possible that the "milking " process could follow the previous digestion by lysosomes i.e. the "farming" process, and not be exclusive of one another. The entire intracellular pathway corresponds to the proposed hypothetical model (Figure 8A) of a downward going cytoplasmic polarity from the apex to the basal lamina and then into the blood that flows below the basal lamina. We suppose this is the natural symbiont and metabolite pathway in *Bathymodiolus azoricus in situ*, where there is a possible continuous supply of symbionts from their environment. During an extended sulfide and methane depletion, we observed extremely large accumulations of symbionts and very large lysosomes. If all these symbionts succeeded to follow the apico-basal pathway until complete digestion, the big lysosome would get empty and likely resorb and disappear. Then at the end of digestion

of the last symbiont, the bacteriocyte would be devoid of symbionts.

The baso-apical return triggered by apoptosis/necroptosis

When digestion is intensive, at d7-d9, it is noteworthy that the microvilli increase both in size and number. They sometimes appear curving toward each other, as if they were to encircle and finally phagocyte a symbiotic bacterium. They correspond to the pit-like structures previously described by Dubilier et al. (1998); Won et al. (2003); Kádár et al. (2006). In the mussels kept in filtered sea-water, the apex of the bacteriocytes gets a spongy appearance with empty vacuoles, as also quoted by Kádár et al. (2005), who supposed that the symbionts could be expelled from the apex. Since Ikuta et al. (2021) recently showed that the apical symbiont-containing vesicles build a network that remains connected to the outside, exocytosis of the symbionts could occur the more easily. However, the apical spongy appearance could also be a sign that endocytosis continues, but that there are no new bacteria to phagocyte, so the newly created vacuoles remain empty. Endocytosis in *Bathymodiolus* has indeed been shown possible during the entire life of the deep-sea mussel (Wentrup et al., 2013) and is first seen at the very initiation of the symbiosis in the larval stage, just after metamorphosis (Laming et al., 2018; Franke et al., 2020).

It is interesting to mention that the epidermal apico-basal cell height does progressively shrink, indicating that the symbionts must be lost at some point. Also, we repeatedly observed missing bacteriocytes in various locations above the basal lamina, but framed by intact intercalary cells. At the base of the missing cells or in the remaining cellular material, we observed nuclear features with very dark condensed chromatin, even in the freshly collected *Bathymodiolus*. We think they correspond to apoptotic nuclei, in accordance with high rates of apoptotic cells recently documented in *B. azoricus*, whatever they were collected with a pressure-maintaining device, or unpressurized (Piquet et al., 2019). As described by Kerr et al. (1972), early apoptosis starts with DNA fragmentation (revealed by the TUNEL assays used in Piquet et al., 2019), followed by chromatin condensation (pycnosis) and nuclear fragmentation (caryorrhexis). Then the plasma membrane starts blebbing, although remaining intact, the cytoplasm shrinks, and finally apoptotic bodies of cytoplasm containing intact organelles and fragments of nuclei are extruded to be phagocyted by other cells. On the contrary, necrosis (the uncontrolled cell death) shows swelling and disruption of both nuclear envelope and plasma membrane, with release of all altered organelles. In *Bathymodiolus* we saw round structures within a continuous envelope generally surrounded by swollen rough endoplasmic reticulum (i.e. at a circum-nuclear position) and having more or less peripheric spots of electron dense material, that looks like pre-apoptotic or apoptotic condensed chromatin (Kerr et al., 1972; Chipuk and Green, 2005; Elmore, 2007). We also saw quite a few plasma membranes blebbing out (although not always remaining intact, but this is often difficult to assess on sections) and we measured a continuous shrinkage of the cells during starvation. We also recorded isolated cytoplasmic bodies containing nuclear fragments expelled out of the gill epidermis, which looked as apoptotic bodies. However, since we also observed modified swollen reticulum and expulsion of isolated vacuoles, it is not possible to rule out it could be necroptosis, another form of regulated cell death involving Receptor-Interacting Protein Kinases and TNF (Tumor Necrosis Factors) (Grootjans et al., 2017). Indeed, this regulated cell death displays some morphological features of both apoptosis and necrosis. Necroptosis shares with apoptosis the chromatin condensation and fragmentation, but the extensive cytoplasmic degeneration and plasma membrane rupture are two characteristics it has in common with necrosis (Günther et al., 2013). In necroptosis the nuclear envelope always remains intact, contrary to necrosis were the nuclei explode (de Torres et al., 1997). As necroptosis is a programmed inflammatory cell death, the rapid release of the cellular content in the environment is acting as a danger or damage-associated molecular patterns attracting immune cells (Grootjans et al., 2017). Interestingly, in *Bathymodiolus* we saw more hemocytes (i.e. immunity cells) filling the hemolymph space after 9 days starvation. With the present data we cannot ascertain, whether we observed apoptosis or necroptosis or both.

Anyway apoptosis/necroptosis could trigger the upward expulsion of the very big lysosomes. The digested material would be flowing out with the gill water flow, up to the mouth and be digested in the stomach. Kádár et al. (2006) found bacteria in the digestive gland, but of course they could also come from the environment, and moreover, undigested symbionts could also just be expelled in the environment.

Epidermis renewal: Back to a regular filter-feeding type of epidermis

In *B. azoricus* we also evidenced cell division in the bacteriocyte zone, where we found apoptosis, indicating a high cellular turnover of the mussel gill epidermis, higher than in non-symbiotic *Mytilus* (Piquet et al., 2020; Piquet et al., 2019). Cellular turnover in mammals skin epidermis is also triggered by apoptosis, and the epidermal cells are regularly replaced by new cells found more basally (Alberts et al., 2002). In the present experiment, we saw that when the bacteriocytes showed apical empty blebbing and were out-pocking above the mean apical level of the epidermis, there were often oblique basal nuclei nearby that in fact belong to the neighboring intercalary cells. Even narrow, these intercalary cells occur to possibly have divided in two

daughter cells, since their nuclei remain so tightly together on each side of the plasma membrane of the intercalary cells to which they belong. Their oblique nucleus and crescent-shape basal cytoplasm suggests a shifting cytoplasmic movement towards the basal lamina and the space where the old bacteriocyte is (or will be) missing. This suggests that intercalary cells could be true stem cells, being able to divide into two daughter cells, one of which remains an intercalary stem-cell, while the other could differentiate into the missing cell-type, thereby filling out the empty space left on the basal lamina and renewing the gill epidermis. We summarized all these cellular steps in our model shown in Figures 8A, B.

After 61 days (i.e. two months starvation) no symbiont occurs in any gill sample. The gill epidermis looks strikingly similar to that of the coastal filter-feeding mussel *M. edulis* having basal nuclei in square shaped cells. This process also involves a general shrinkage of the apico-basal axis of epithelial cells, suggesting that the decrease in volume of cells is associated with the progressive loss of symbionts. During the starvation experiment, apical microvilli develop that were absent in symbiont-loaded cells. Altogether these observations suggest that a given bacteriocyte actually loses its bacteria upon starvation, and the host cells might be destroyed by apoptosis/necroptosis. Finally, the epidermis might be renewed by the intercalary stem cell divisions. The epidermal cells could have the plasticity to filter-feed, thus ensuring mussel's heterotrophic nutrition at least temporarily, in a way similar to that suggested during the pelagic larval phase (Laming et al., 2018). To which extent this epithelium is efficient for filter-feeding is not fully understood (Page et al., 1991; Page et al., 1990; Riou et al., 2010), but this could allow mussels to survive during extended episodes of vent fluid extinction.

Whether and how fast these new undifferentiated, symbiont-free, epidermal cells are able to reacquire symbionts from their surroundings, remains to be investigated. Such as it has been done in *Codakia orbiculata* and *Lucina pensylvanica*, two other symbiotic bivalves (Elisabeth et al., 2014), that rebuild a fully functional symbiont-loaded gill. It would be interesting to test whether released symbionts can occur in the seawater around starving *Bathymodiolus*, and to incubate symbiont-depleted mussels in symbiont-containing water or in the presence of symbiont-bearing hosts. Another important step would be to ascertain the origin of undifferentiated epithelial cells and of bacteriocytes. For this, EdU labeling should be used to mark cells that have undergone division, and correlative microscopy could be used to test, whether intercalary cells do divide and produce epithelial daughter cells, which would confirm their role as stem cells in the deep-sea mussel gill epidermis. For sure, some cell plasticity in the gills, their main feeding organ, must account for the extraordinary long resistance of the deep-sea mussel in non-vent seawater.

Data availability statement

The raw data supporting the conclusions of this article can be made available by the authors, without undue reservation.

Author contributions

BP has acquired and preserved the mussel samplings during the cruises MOMARSAT and BIOBAZ (2017), and conducted all the experiments. AA and SP has helped with section-cutting and TEM microphotographs. FL has organized BioBaz-cruise and helped on board with fixations and mussel recovery from Azores to France. BP, AA, and SD have together designed the experiments. SD and AA have tutored BP during her laboratory experiments, in Paris and Roscoff respectively. AA wrote the paper from an initial French version of BP's pHD, and all authors read and improved the text after fruitful discussions.

Funding

This work could not have been done without the joint grants from the Region Bretagne, for the project FlexSyBi, and the financial support from the Institut Universitaire de France for the laboratory work during the pHD of Bérénice Piquet (Grant number COH15020). The funders had no role in study design, data collection and analysis, decision to publish, nor preparation of the manuscript. All results are issued from the pHD of Bérénice Piquet, defended in Roscoff on the 23th Oktober 2018.

Acknowledgments

The authors wish to thank the Captain and crews of the cruises MOMARSAT 2017 and BioBaz 2017 for the mussel samplings and laboratory facilities. We thank Lab Horta for welcoming us after the Cruise. We are grateful to Océanopolis aquaria in Brest and Roscoff Aquarium Service to have welcomed and kept the deep-sea and coastal mussels. Finally, we thank the microscopy platform Merimage (Roscoff, France) partner core facilities and the Institute of Biology Paris-Seine Imaging Facility, supported by the "Conseil Regional Ile-de France", CNRS and Sorbonne Université. The authors also

wish to thank François Vandenbosch for the video (in Supplementary Material).

Conflict of interest

The authors declare that the research was conducted in the absence of any commercial or financial relationships that could be construed as a potential conflict of interest.

Publisher's note

All claims expressed in this article are solely those of the authors and do not necessarily represent those of their affiliated organizations, or those of the publisher, the editors and the reviewers. Any product that may be evaluated in this article, or claim that may be made by its manufacturer, is not guaranteed or endorsed by the publisher.

Supplementary material

The Supplementary Material for this article can be found online at: https://www.frontiersin.org/articles/10.3389/fmars.2022.968331/full#supplementary-material

SUPPLEMENTARY VIDEO

Moving *Bathymodiolus* in their aquaria during starvation. The deep-sea mussels kept in filtered sea-water during the entire experiment show they are actively creeping on the walls of the aquaria by extending their foot. They also expand their siphons. The video is filmed with an Olympus E-620 with the objective Olympus Zuiko Digital ED 14-42 mm and accelerated x 450 times.

References

Alberts, B., Johnson, A., Lewis, J., Raff, M., Roberts, K., and Walter, P. (2002). *Molecular biology of the cell*. 4th edn. New York: Garland Science. 1616 pp.

Arends, F., and Lieleg, O. (2016). "Biophysical properties of the basal lamina: A highly selective extracellular matrix," In composition and function of the extracellular matrix in the human body. *IntechOpen*. 374 pp. doi: 10.5772/62519

Assié, A., Borowski, C., van der Heijden, K., Raggi, L., Geier, B., Leisch, N., et al. (2016). A specific and widespread association between deep-sea *Bathymodiolus* mussels and a novel family of epsilonproteobacteria: Epsilonproteobacterial epibiont Of *Bathymodiolus*. *Environ. Microbiol. Rep.* 8, 805–813. doi: 10.1111/1758-2229.12442

Bettencourt, R., Dando, P., Rosa, D., Riou, V., Colaço, A., Sarrazin, J., et al. (2008). Changes of gill and hemocyte-related bio-indicators during long term maintenance of the vent mussel bathymodiolus azoricus held in aquaria at atmospheric pressure. *Comp. Biochem. Physiol. A. Mol. Integr. Physiol.* 150, 1–7. doi: 10.1016/j.cbpa.2008.02.020

Brooks, J. M., Kennicutt, M. C., Fisher, C. R., Macko, S. A., Cole, K., Childress, J. J., et al. (1987). Deep-Sea hydrocarbon seep communities: Evidence for energy and nutritional carbon sources. *Science* 238, 1138–1142. doi: 10.1126/science.238.4830.1138

Cavanaugh, C. M., Wirsen, C. O., and Jannasch, H. W. (1992). Evidence for methylotrophic symbionts in a hydrothermal vent mussel (Bivalvia: Mytilidae) from the mid-Atlantic ridge. *Appl. Environ. Microbiol.* 58, 3799–3803. Available at: 0099-2240/92/123799-05$02.00/0

Childress, J. J., Fisher, C. R., Brooks, J. M., Kennicutt, M. C., Bidigare, R. R., and Anderson, A. C. (1986). A methanotrophic marine molluscan (Bivalvia, mytilidae) symbiosis : Mussels fueled by gas. *Science* 233, 1306–1308. Available at: https://www.jstor.org/stable/1697981

Chipuk, J. E., and Green, D. R. (2005). Do inducers of apoptosis trigger caspase-independent cell death? *Nat. Rev. Mol. Cell Biol.* 6, 268–275. doi: 10.1038/nrm1573

Colaço, A., Desbruyères, D., Comtet, T., and Alayse, A.-M. (1998). Ecology of the menez Gwen hydrothermal vent field (Mid-Atlantic Ridge/Azores triple junction). *Cah. Biol. Mar.* 39, 237–240. doi: 10.21411/CBM.A.3D6E4229

de Torres, C., Munell, F., Ferrer, I., Reventos, J., and Macaya, A. (1997). Identification of necrotic cell death by the TUNEL assay in the hypoxic-ischemic neonatal rat brain. *Neurosci. Lett.* 230, 1–4. doi: 10.1016/S0304-3940(97)00445-X

Détrée, C., Lallier, F. H., Tanguy, A., and Mary, J. (2017). Identification and gene expression of multiple peptidoglycan recognition proteins (PGRPs) in the deep-sea mussel *Bathymodiolus azoricus*, involvement in symbiosis? *Comp. Biochem. Physiol. B Biochem. Mol. Biol.* 207, 1–8. doi: 10.1016/j.cbpb.2017.02.002

Distel, D. L., Baco, A. R., Chuang, E., Morrill, W., Cavanaugh, C., and Smith, C. R. (2000). Do mussels take wooden steps to deep-sea vents? *Mar. ecology. Nat.* 403, 725–726. doi: 10.1038/35001667

Dubilier, N., Windoffer, R., and Giere, O. (1998). Ultrastructure and stable carbon isotope composition of the hydrothermal vent mussels bathymodiolus brevior and b. sp. affinis brevior from the north Fiji basin, western pacific. *Mar. Ecol. Prog. Ser.* 165, 187–193. doi: 10.3354/meps165187

Duperron, S. (2010). "The diversity of deep-sea mussels and their bacterial symbioses," in *The vent and seep biota*. Ed. S. Kiel (Dordrecht: Springer), 137–167.

Duperron, S., Bergin, C., Zielinski, F., Blazejak, A., Pernthaler, A., McKiness, Z. P., et al. (2006). A dual symbiosis shared by two mussel species, *Bathymodiolus azoricus* and *Bathymodiolus puteoserpentis* (Bivalvia: Mytilidae), from hydrothermal vents along the northern mid-Atlantic ridge. *Environ. Microbiol.* 8, 1441–1447. doi: 10.1111/j.1462-2920.2006.01038.x

Duperron, S., Halary, S., Lorion, J., Sibuet, M., and Gaill, F. (2008). Unexpected co-occurrence of six bacterial symbionts in the gills of the cold seep mussel *Idas* sp. (Bivalvia: Mytilidae). *Environ. Microbiol.* 10, 433–445. doi: 10.1111/j.1462-2920.2007.01465.x

Duperron, S., Nadalig, T., Caprais, J.-C., Sibuet, M., Fiala-Medioni, A., Amann, R., et al. (2005). Dual symbiosis in a *Bathymodiolus* sp. mussel from a methane seep on the Gabon continental margin (Southeast atlantic): 16S rRNA phylogeny and distribution of the symbionts in gills. *Appl. Environ. Microbiol.* 71, 1694–1700. doi: 10.1128/AEM.71.4.1694-1700.2005

Duperron, S., Quiles, A., Szafranski, K. M., Léger, N., and Shillito, B. (2016). Estimating symbiont abundances and gill surface areas in specimens of the hydrothermal vent mussel *Bathymodiolus puteoserpentis* maintained in pressure vessels. *Front. Mar. Sci.* 3. doi: 10.3389/fmars.2016.00016

Elisabeth, N. H., Caro, A., Césaire, T., Mansot, J.-L., Escalas, A., Sylvestre, M.-N., et al. (2014). Comparative modifications in bacterial gill-endosymbiotic populations of the two bivalves *Codakia orbiculata* and *Lucina pensylvanica* during bacterial loss and reacquisition. *FEMS Microbiol. Ecol.* 89, 646–658. doi: 10.1111/1574-6941.12366

Elmore, S. (2007). Apoptosis: a review of programmed cell death. *Toxicol. Pathol.* 35, 495–516. doi: 10.1080/01926230701320337

Fiala-Medioni, A., Michalski, J.-C., Jollès, J., Alonso, C., and Montreuil, J. (1994). Lysosomic and lysozyme activities in the gill of bivalves from deep hydrothermal vents. *Comptes Rendus Académie Sci. Paris* 317, 239–244.Available at: http://pascal-francis.inist.fr/vibad/index.php?action=getRecordDetail&idt=4051660

Fisher, C. R., and Childress, J. J. (1992). Organic carbon transfer from methanotrophic symbionts to the host hydrocarbon-seep mussel. *Symbiosis* 12, 221–235. Available at: 0334-5114/92 /$03.50 @1992

Fisher, C. R., Childress, J. J., Oremland, R. S., and Bidigare, R. R. (1987). The importance of methane and thiosulfate in the metabolism of the bacterial symbionts of two deep-sea mussels. *Mar. Biol.* 96, 59–71. doi: 10.1007/BF00394838

Franke, M., Geier, B., Hammel, J. U., Dubilier, N., and Leisch, N. (2020). Coming together – symbiont acquisition and early development of *Bathymodiolus* mussels. *Proc. R. Soc. B* 10, 288202110442021044. doi: 10.1101/ 2020.10.09.333211

Fujiwara, Y., Kawato, M., Noda, C., Kinoshita, G., Yamanaka, T., Fujita, Y., et al. (2010). Extracellular and mixotrophic symbiosis in the whale-fall mussel adipicola pacifica: A trend in evolution from extra- to intracellular symbiosis. *PLoS One* 5, e11808. doi: 10.1371/journal.pone.0011808

Grootjans, S., Vanden Berghe, T., and Vandenabeele, P. (2017). Initiation and execution mechanisms of necroptosis: an overview. *Cell Death Differ* 24, 1184–1195. doi: 10.1038/cdd.2017.65

Günther, C., Neumann, H., Neurath, M. F., and Becker, C. (2013). Apoptosis, necrosis and necroptosis: cell death regulation in the intestinal epithelium. *Gut* 62, 1062–1071. doi: 10.1136/gutjnl-2011-301364

Halary, S., Duperron, S., and Boudier, T. (2011). Direct image-based correlative microscopy technique for coupling identification and structural investigation of bacterial symbionts associated with metazoans. *Appl. Environ. Microbiol.* 77, 4172–4179. doi: 10.1128/AEM.02461-10

Ikuta, T., Amari, Y., Tame, A., Takaki, Y., Tsuda, M., Iizuka, R., et al. (2021). Inside or out? clonal thiotrophic symbiont populations occupy deep-sea mussel bacteriocytes with pathways connecting to the external environment. *ISME Commun.* 1, 38. doi: 10.1038/s43705-021-00043-x

Kádár, E., Bettencourt, R., Costa, V., Santos, R. S., Lobo-da-Cunha, A., and Dando, P. (2005). Experimentally induced endosymbiont loss and re-acquirement in the hydrothermal vent bivalve bathymodiolus azoricus. *J. Exp. Mar. Biol. Ecol.* 318, 99–110. doi: 10.1016/j.jembe.2004.12.025

Kádár, E., Davis, S. A., and Lobo-da-Cunha, A. (2008). Cytoenzymatic investigation of intracellular digestion in the symbiont-bearing hydrothermal bivalve *Bathymodiolus azoricus*. *Mar. Biol.* 153, 995–1004. doi: 10.1007/s00227-007-0872-0

Kádár, E., Santos, R. S., and Powell, J. J. (2006). Biological factors influencing tissue compartmentalization of trace metals in the deep-sea hydrothermal vent bivalve *Bathymodiolus azoricus* at geochemically distinct vent sites of the mid-Atlantic ridge. *Environ. Res.* 101, 221–229. doi: 10.1016/j.envres.2005.08.010

Kerr, J. F. R., Wyllie, A. H., and Currie, A. R. (1972). Apoptosis: a basic biological phenomenon with wide-ranging implications in tissue kinetics. *Br. J. Cancer* 26, 239–257. Available at: https://www.nature.com/articles/bjc197233

Lallier, F. H. (2017). BIOBAZ 2017 cruise, RV Pourquoi pas? doi: 10.17600/17014600

Laming, S. R., Gaudron, S. M., and Duperron, S. (2018). Lifecycle ecology of deep-Sea chemosymbiotic mussels: A review. *Front. Mar. Sci.* 5. doi: 10.3389/fmars.2018.00282

Le Pennec, M., Diouris, M., and Herry, A. (1988). Endocytosis and lysis of bacteria in gill epithelium of bathymodiolus thermophilus, *Thyasira flexuosa* and *Lucinella divaricata* (Bivalave, molluscs). *J. Shellfish Res.* 7, 483–489. Available at: https://www.biodiversitylibrary.org/page/2150100

Little, C. T. S., and Vrijenhoek, R. C. (2003). Are hydrothermal vent animals living fossils? *Trends Ecol. Evol.* 18, 582–588. doi: 10.1016/j.tree.2003.08.009

Lorion, J., Kiel, S., Faure, B., Kawato, M., Ho, S. Y. W., Marshall, B., et al. (2013). Adaptive radiation of chemosymbiotic deep-sea mussels. *Proc. R. Soc B Biol. Sci.* 280, 20131243–20131243. doi: 10.1098/rspb.2013.1243

Muscatine, L., McCloskey, R., and Marian, E. R. (1981). Estimating the daily contribution of carbon from zooxanthellae to coral animal respiration1: Muscatine et al. *Limnol. Oceanogr* 26, 601–611. doi: 10.4319/lo.1981.26.4.0601

Page, H. M., Fiala-Medioni, A., Fisher, C. R., and Childress, J. J. (1991). Experimental evidence for filter-feeding by the hydrothermal vent mussel, *Bathymodiolus thermophilus*. *Deep Sea Res. Part Oceanogr. Res. Pap* 38, 1455–1461. doi: 10.1016/0198-0149(91)90084-S

Page, H. M., Fisher, C. R., and Childress, J. J. (1990). Role of filter-feeding in the nutritional biology of a deep-sea mussel with methanotrophic symbionts. *Mar. Biol.* 104, 251–257. doi: 10.1007/BF01313266

Piquet, B. (2018). *La flexibilité des symbioses entre bivalves et bactéries chimiotrophes : mécanismes, régulation et résilience* (Paris (France: Sorbonne University).

Piquet, B., Lallier, F. H., André, C., Shillito, B., Andersen, A. C., and Duperron, S. (2020). Regionalized cell proliferation in the symbiont-bearing gill of the hydrothermal vent mussel bathymodiolus azoricus. *Symbiosis* 82, 225–233. doi: 10.1007/s13199-020-00720-w

Piquet, B., Shillito, B., Lallier, F. H., Duperron, S., and Andersen, A. C. (2019). High rates of apoptosis visualized in the symbiont-bearing gills of deep-sea bathymodiolus mussels. *PLoS One* 14, e0211499. doi: 10.1371/journal.pone.0211499

Raggi, L., Schubotz, F., Hinrichs, K.-U., Dubilier, N., and Petersen, J. M. (2013). Bacterial symbionts of *Bathymodiolus* mussels and *Escarpia* tubeworms from chapopote, an asphalt seep in the southern gulf of Mexico: Chapopote *Bathymodiolus* and *Escarpia* symbioses. *Environ. Microbiol.* 15, 1969–1987. doi: 10.1111/1462-2920.12051

Riou, V., Colaço, A., Bouillon, S., Khripounoff, A., Dando, P., Mangion, P., et al. (2010). Mixotrophy in the deep sea: a dual endosymbiotic hydrothermal mytilid assimilates dissolved and particulate organic matter. *Mar. Ecol. Prog. Ser.* 405, 187–201. doi: 10.3354/meps08515

Sarradin, P.-M., and Cannat, M. (2017). MOMARSAT2017 cruise, Pourquoi pas ? R/V (Sismer). doi: 10.17600/17000500

Shin, K., Fogg, V. C., and Margolis, B. (2006). Tight junctions and cell polarity. *Annu. Rev. Cell Dev. Biol.* 22, 207–235. doi: 10.1146/annurev.cellbio.22.010305.104219

Streams, M. E., Fisher, C. R., and Fiala-Medioni, A. (1997). Methanotrophic symbiont location and fate of carbon incorporated from methane in a hydrocarbon seep mussel. *Mar. Biol.* 129, 465–476. Available at: https://link.springer.com/article/10.1007/s002270050187

Sun, Y., Wang, M., Li, L., Zhou, L., Wang, X., Zheng, P., et al. (2017). Molecular identification of methane monooxygenase and quantitative analysis of methanotrophic endosymbionts under laboratory maintenance in *Bathymodiolus platifrons*From the south China Sea. *PeerJ* 5, e3565. doi: 10.7717/peerj.3565

Szafranski, K. M., Piquet, B., Shillito, B., Lallier, F. H., and Duperron, S. (2015). Relative abundances of methane- and sulfur-oxidizing symbionts in gills of the deep-sea hydrothermal vent mussel *Bathymodiolus azoricus* under pressure. *Deep Sea Res. Part Oceanogr. Res. Pap* 101, 7–13. doi: 10.1016/j.dsr.2015.03.003

Tame, A., Maruyama, T., and Yoshida, T. (2022). Phagocytosis of exogenous bacteria by gill epithelial cells in the deep-sea symbiotic mussel *Bathymodiolus japonicus*. *R. Soc Open Sci.* 9, 211384. doi: 10.1098/rsos.211384

Wentrup, C., Wendeberg, A., Huang, J. Y., Borowski, C., and Dubilier, N. (2013). Shift from widespread symbiont infection of host tissues to specific colonization of gills in juvenile deep-sea mussels. *ISME J.* 7, 1244–1247. doi: 10.1038/ismej.2013.5

Wentrup, C., Wendeberg, A., Schimak, M., Borowski, C., and Dubilier, N. (2014). Forever competent: deep-sea bivalves are colonized by their chemosynthetic symbionts throughout their lifetime: Symbiont colonization in gills of deep-sea bivalves. *Environ. Microbiol.* 16, 3699–3713. doi: 10.1111/1462-2920.12597

Won, Y.-J., Hallam, S. J., O'Mullan, G. D., Pan, I. L., Buck, K. R., and Vrijenhoek, R. C. (2003). Environmental acquisition of thiotrophic endosymbionts by deep-sea mussels of the genus *Bathymodiolus*. *Appl. Environ. Microbiol.* 69, 6785–6792. doi: 10.1128/AEM.69.11.6785-6792.2003

Zielinski, F. U., Pernthaler, A., Duperron, S., Raggi, L., Giere, O., Borowski, C., et al. (2009). Widespread occurrence of an intranuclear bacterial parasite in vent and seep bathymodiolin mussels. *Environ. Microbiol.* 11, 1150–1167. doi: 10.1111/j.1462-2920.2008.01847.x